DNA-TR-84-388

AN ANALYSIS OF ARMY THERMAL TRANSMISSIVITY CALCULATIONS

Kaman Sciences Corporation Systems Directorate
1911 Jefferson Davis Highway
Arlington, VA 22202-3508

1 November 1984

Technical Report

CONTRACT No. DNA 001-83-C-0232

THIS WORK WAS SPONSORED BY THE DEFENSE NUCLEAR AGENCY
UNDER RDT&E RMSS CODE B342083466 N99QAXAT00001 H2590D.

Prepared for
Director
DEFENSE NUCLEAR AGENCY
Washington, DC 20305-1000

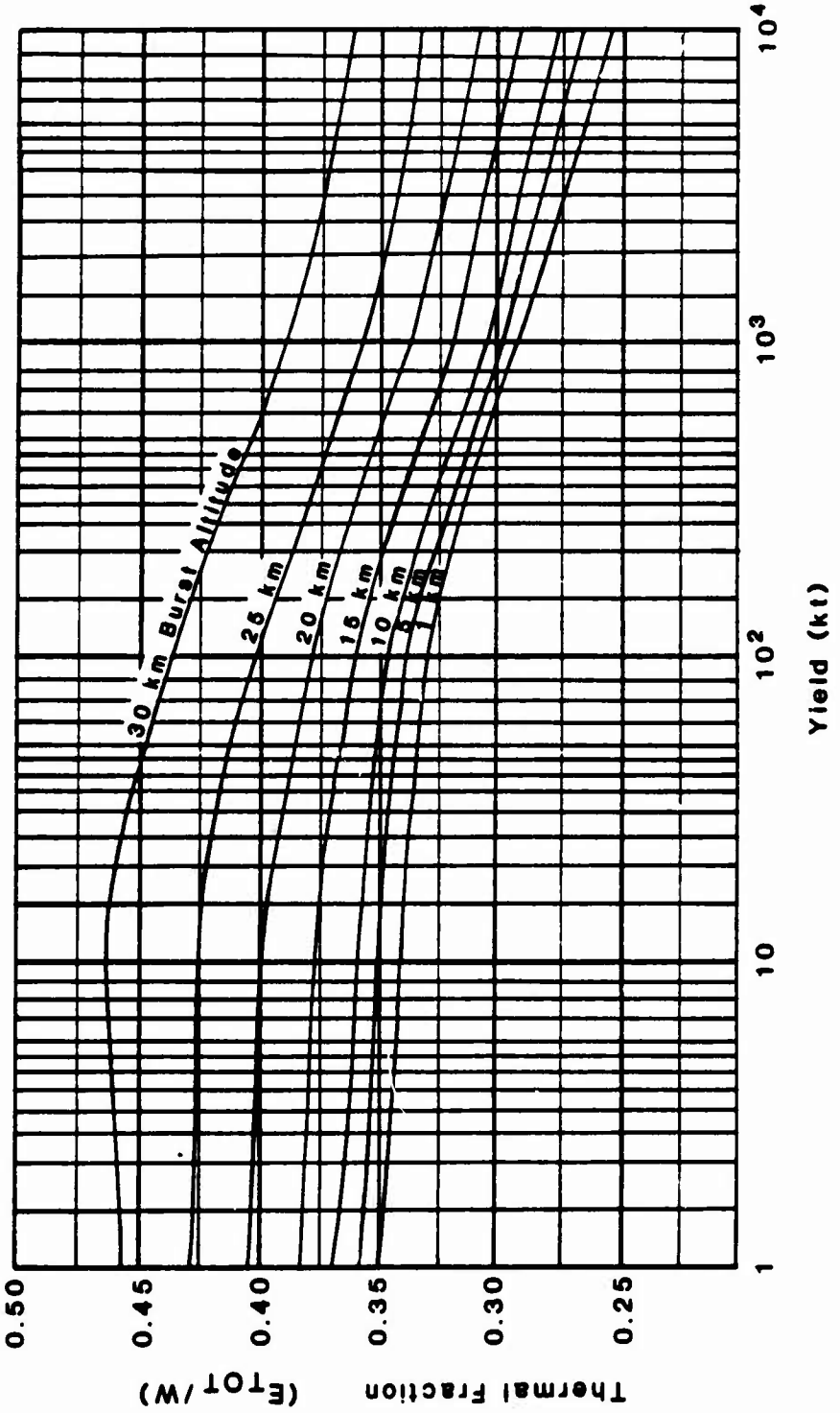

Figure 12. Thermal Yield Fraction as a Function of Burst Altitude and Yield (Yield Contours)
(Source: Hillendahl, 1980; EM-1 Date: February 1982)

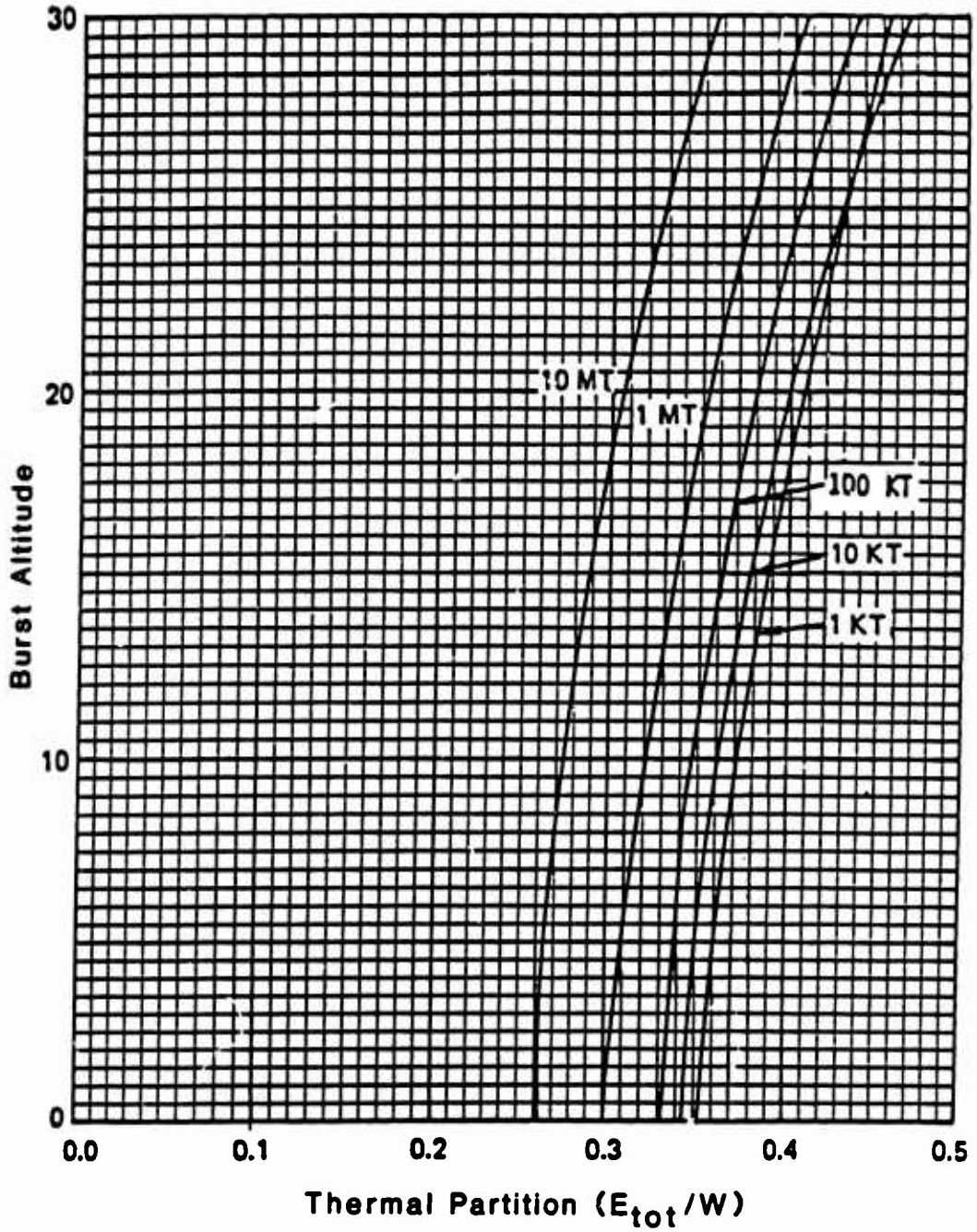

Figure 13. Thermal Yield Fraction as a Function of Burst Altitude and Yield (Altitude Contours)
(Source: Hillendahl, 1980: EM-1 Date: February 1982)

Table 6. Thermal Partition for Near-Surface Bursts.

Yield (KT)	Surface Burst Partition (Fraction)	Non-Surface Burst Partition (Fraction)	Transition Height (Meters)
1	0.045	0.350	4
10	0.066	0.341	8.6
100	0.13	0.330	18.5
1000	0.16	0.291	40
10000	0.17	0.254	86

The difference noted for the surface and non-surface bursts have major implications in predictions of the exposure from low altitude bursts especially for receivers near the ground surface. For lower yield tactical devices the thermal output of a surface burst is 1/3 that of a low altitude free air burst for a 100 kt yield. For a 1 kt yield the ratio is about 1/8. A shape factor must also be considered since the fireballs for the interacting bursts are strongly perturbed and are hemispherical in shape. Examples of the magnitude of these effects on the exposure predictions will be considered in the following sections.

3.1.2 Time Dependent Power.

Previous USANCA thermal prediction methods have ignored time dependent effects. For many applications and certainly for any detailed response calculations the time dependence of the thermal environment is very important. For eye damage effects and especially for evaluation of eye protective devices, the time dependence of the radiant level is very important. The RECIPE

code gives the time dependent fireball power output in detail including a general representation of the first pulse as discussed previously, a classified version is available giving the first pulse in detail.

The basic output of the SPFLUX routine is the spectral power FOLZ(H) (w/eV) as a function of photon energy at the time of interest. The shape factor (SAF) is then applied to obtain the power emitted in a particular receiver direction

$$FOLZH(h\nu) = FOLZ(h\nu) * SAF. \tag{16}$$

Two alternate time dependent modes are available. In one mode a time mesh is defined and the above spectral power is stored for each of the time steps for use in the predictive routines of TAXV. More detail about this mode will be given later. In the other mode, the calculation above is completed for each single time step defined by the TAXV control routine of interest.

The power is then obtained as a function of time by summation over the energy intervals

$$P(t) = \sum_{h\nu} FOLZH(h\nu) * \Delta h\nu \ . \tag{17}$$

As will be discussed in the following section the spectral power is actually converted to a wavelength dependence prior to regrouping into the wavelength mesh used in the transmission routines and further processed into the standard TAXV wavelength grid. In Figure 14 are shown the powertime curves for 100 kt burst for various source altitudes. As discussed previously the unclassified version of RECIPE has been used in this development so the first pulse represents only the continuum contribution from the heated shock. The details of the NO_2 absorption and its

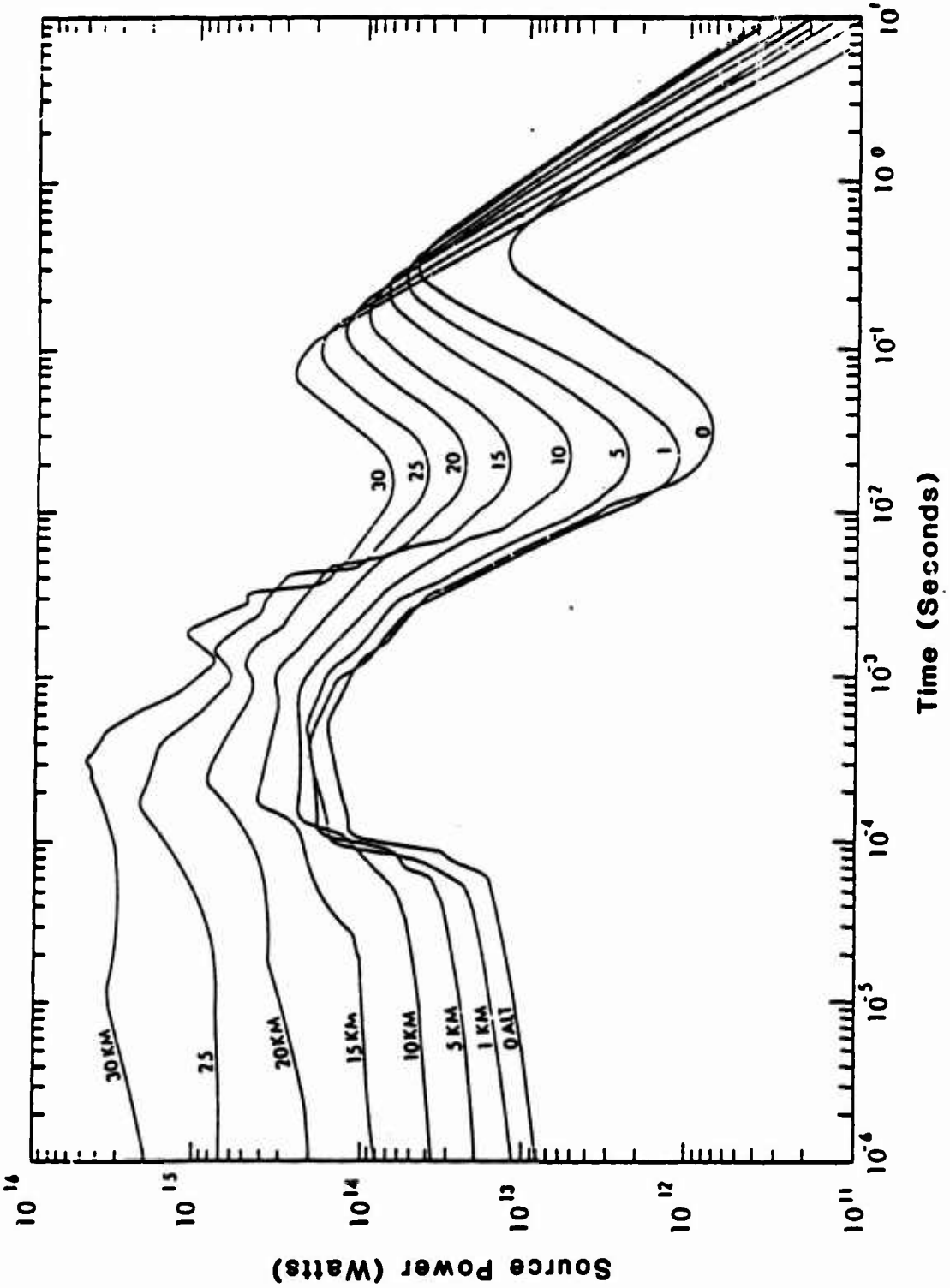

Figure 14. Effect of Altitude on Total Thermal Power, 100-Kiloton Burst.

effect on the early time signature are not included. This is not important for material response considerations since only a very small fraction of the energy is contained in the early pulse.

These curves show the expected trends with altitude. The power level of the first pulse increases with increasing altitude, the minimum is shallower as the altitude is increased, and the second pulse becomes narrower and higher as the altitude increases. Note, the relatively large difference between the free air burst at 1 km and the surface burst. The surface burst has a much smaller second thermal power maximum and a somewhat longer time to second maximum, T2MAX. The first pulse for the two cases is seen to be very similar. These curves represent the power leaving the fireball surface. In order to compute the irradiance at a receiver it is necessary to weight the FOLZS by the atmospheric transmission and the spectral dependent response function before summing over the wavelength bands. This will be discussed in later sections.

This option of computing the response involves accessing the RECIPE routines at each of the times required in the TAXV control routines which can become a relatively time consuming process. Another option mentioned earlier involves generating the matrix FOLZH ($h\nu$,t) for the 26 energy mesh points and a predetermined time grid. The total exposure is then found by integrating over the time grid.

The time mesh is determined in the following manner. A total of 95 time factors are defined with 60 factors increasing in increments from .05 to 3., then with 35 factors increasing in increments of .2 from 3.2 to 10. The actual times are then found by multiplying the time factors by the time of second maximum. In this manner fine time steps are defined from zero to 3 times

the time of second maximum where the power is a rapidly varying function of time. The log-log scales in Figure 14 do not give a good feel for the actual time dependence of the power curves for the second pulse. In Figure 15 the power-time curves in Figure 14 are replotted on normalized linear scales. The abscissa is the ratio of the time to T2MAX. The second thermal pulse when plotted in this normalized manner is seen to display a relatively small altitude dependence. The increase in the minimum power at higher altitudes is shown, and the relative unimportance of the first pulse in terms of total power is shown.

In Figure 16 the irradiance is shown for bursts at an altitude of 1 kft. The receiver is at an altitude of 1 kft and at a range of 31 kft for the 1Mt and at 21 kft for the 100 kt. The total exposure for both cases is 20 cal/cm^2. The data points are the times at which TAXV computes the power time mesh and are seen to represent the shape of the curves in fine detail.

The code does not contain an explicit formula for the total power integrated over the spectrum at T2MAX nor for T2MAX itself. Instead curve fits are used in the code for each of the 26 energy grid points. The expression is of the form:

$$T2MAX(h\nu) = 3.682E\text{-}2 * (W^{**}C(h\nu)) * (\rho/\rho_o)^{**}.315 \qquad (18)$$

where the parameter C is a function of $h\nu$, and the altitude dependence is given by the density ratio expression. The above formula is used if bomb mass is less than 2.5E3 lb/kt. For heavier bombs, a factor involving bomb mass is included which increases T2MAX. In the routines developed for this program T2MAX for the total integrated power is represented by T2MAX for 550 nm since the spectrum tends to be peaked in the visible portion of the spectrum.

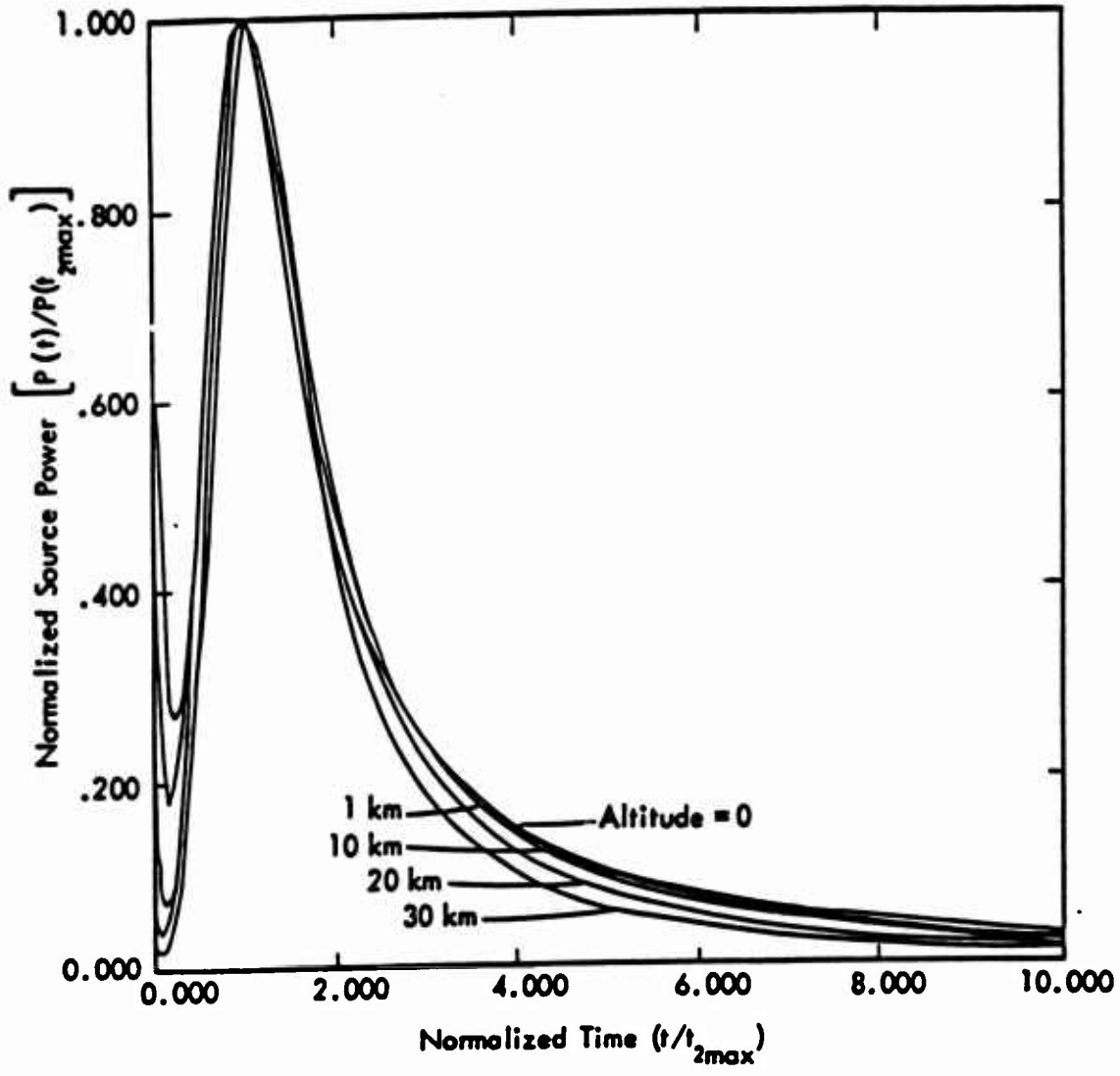

Figure 15. Effect of Altitude on Thermal Power Pulse Shape, 100 Kilotons.

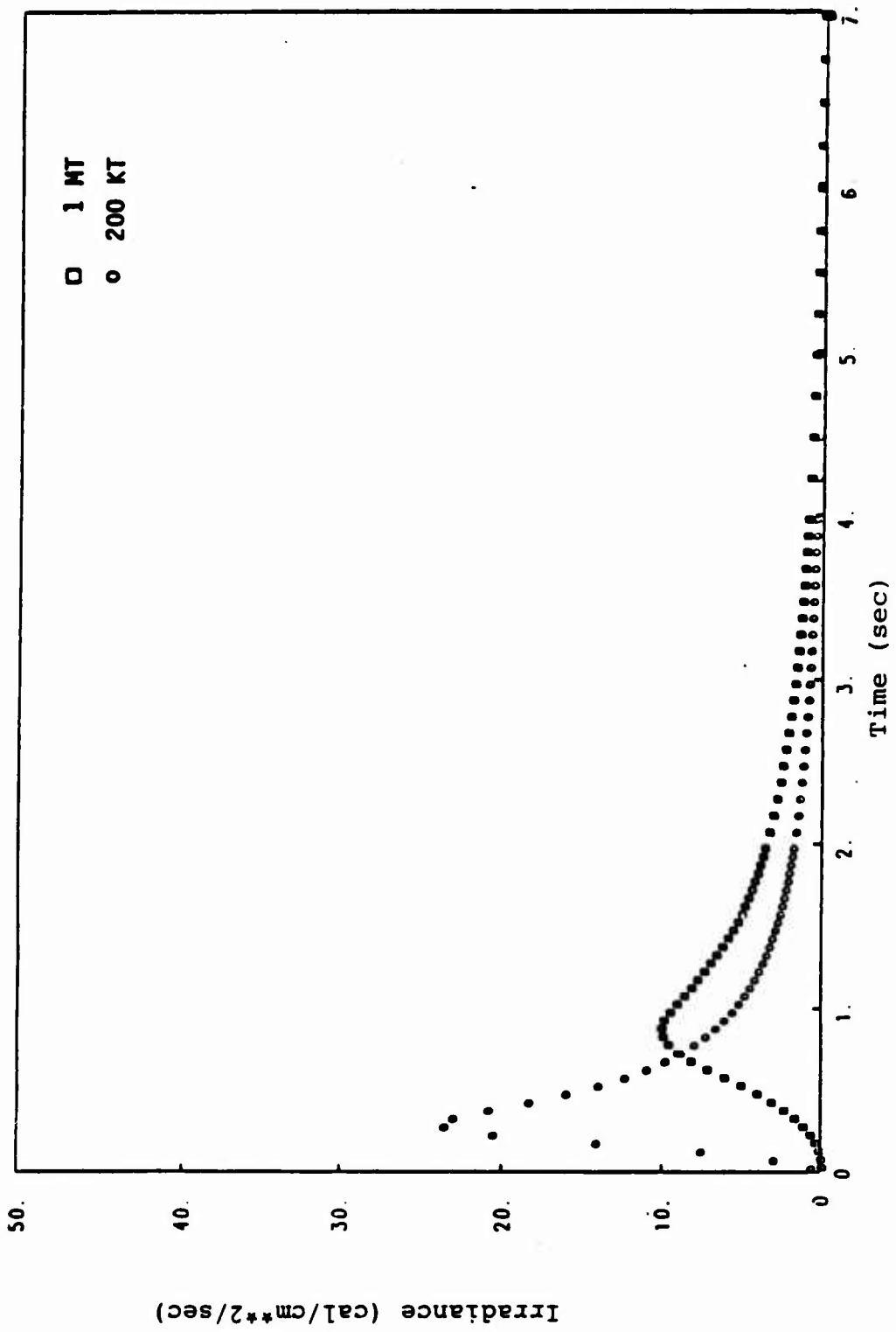

Figure 16. Irradiance Predicted with the Standard Time Factor Mesh for Bursts at 1 KFT Altitude Coaltitude at the 20 Cal/CM² Exposure Level.

3.1.3 Spectral Dependence.

Previous USANCA prediction techniques have not explicitly addressed the spectral dependence of the thermal energy. The spectral distribution of the power from the fireball is of importance primarily for determining the atmospheric transmission from the fireball to the receiver and also to a lesser extent in determining the absorptivity of the material.

As was discussed in the last section, the spectral dependence of the power in RECIPE is described by 26 energy groups which span the wavelength range from 200 to 12500 nm. All of the curve fitting in the code is done as a function of these energy groups and the basic power matrices are developed with the units of watts per eV. These spectral power matrices are used to compute the energy in calories per second in each wavelength band before being combined with the atmospheric transmission factor and the spectral response functions in order to calculate the total energy deposited in the material of interest.

In Figure 17 the spectral distribution is shown for 100 kt burst at several burst altitudes. These curves are obtained by integrating the power matrices over time and represent the distribution for the total energy radiated from the fireball. Each curve has been normalized to unity. The free air bursts all have essentially the same distribution except the bursts at higher altitudes tend to be more sharply peaked and contain more energy in the UV portion of the spectrum. The surface burst is seen to be definitely shifted to longer wavelengths indicating the effects of the ground surface on reducing the radiating temperature of the fireball and the increased absorption from the entrained material. Most of the energy is concentrated in the visible portion of the spectrum with a small fraction having a wavelength greater than one micron.

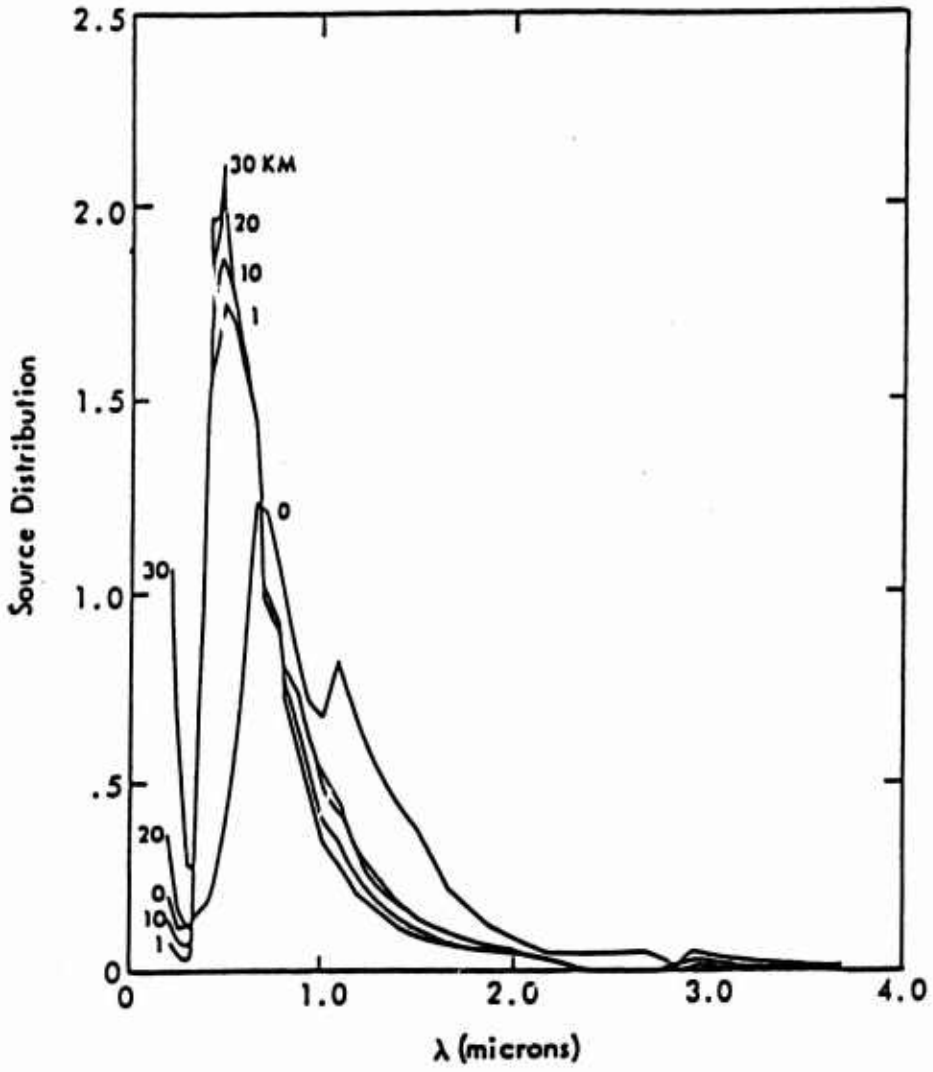

Figure 17. Effect of Altitude on Spectral Distribution, 100 Kilotons.

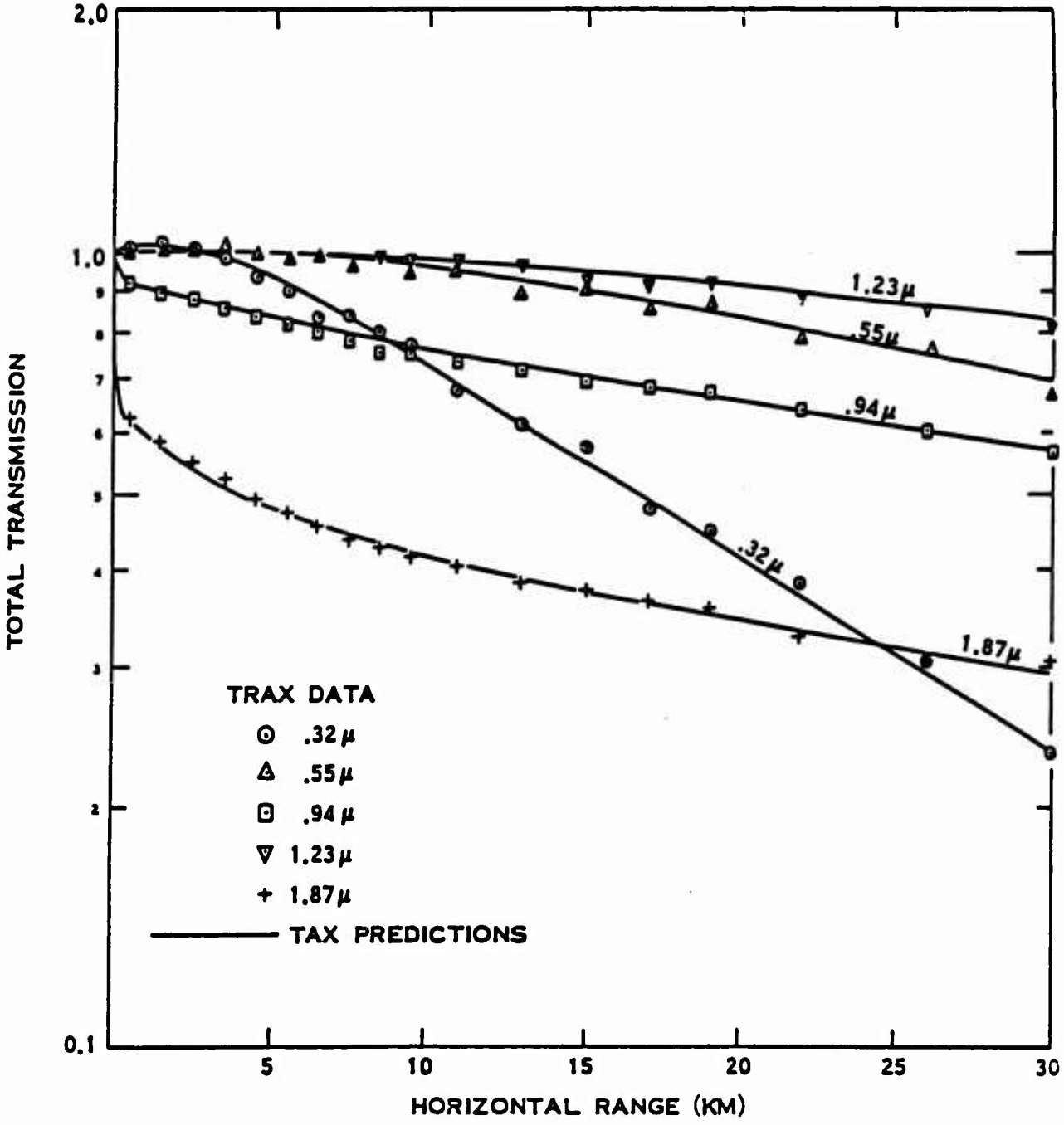

Figure 21. Comparison of Tax Results with TRAX Data Nevada Atmosphere with Ground Level at 1.28 KM Source 1 KM Above Ground. Receiver 3 M Above Ground.

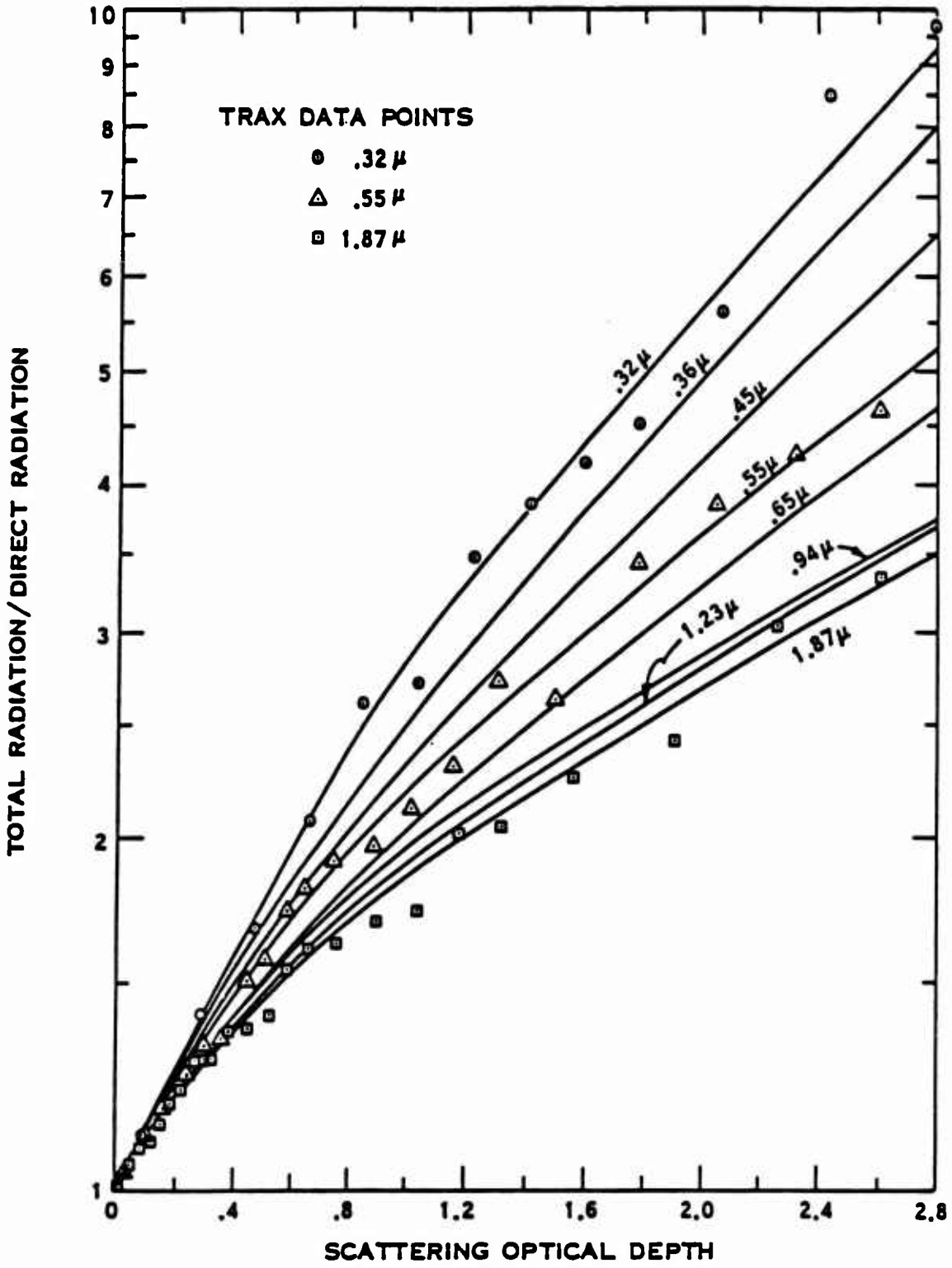

Figure 22. Comparison of Build-up Factors vs the Scattering Optical Depth for Various Wavelengths. Pacific Atmosphere with Both Source and Sampling at 1 km Altitude.

Table 19. Transmission Run Parameters.

YIELDS: 10KT, 100KT

GROUND ALBEDO: ZERO, DIRT, SNOW

CLOUD BASE ALTITUDES: NONE, .3, 1.5, 3.0 KM

SPECTRA: SURFACE, FREE AIR

SOURCE ALTITUDE: ZERO, 1KM

VISIBILITY: 25KM, 6.5KM

RECEIVER: FLAT PLATE ON GROUND FACING SOURCE

HUMIDITY: 1.5, 10G/M^3

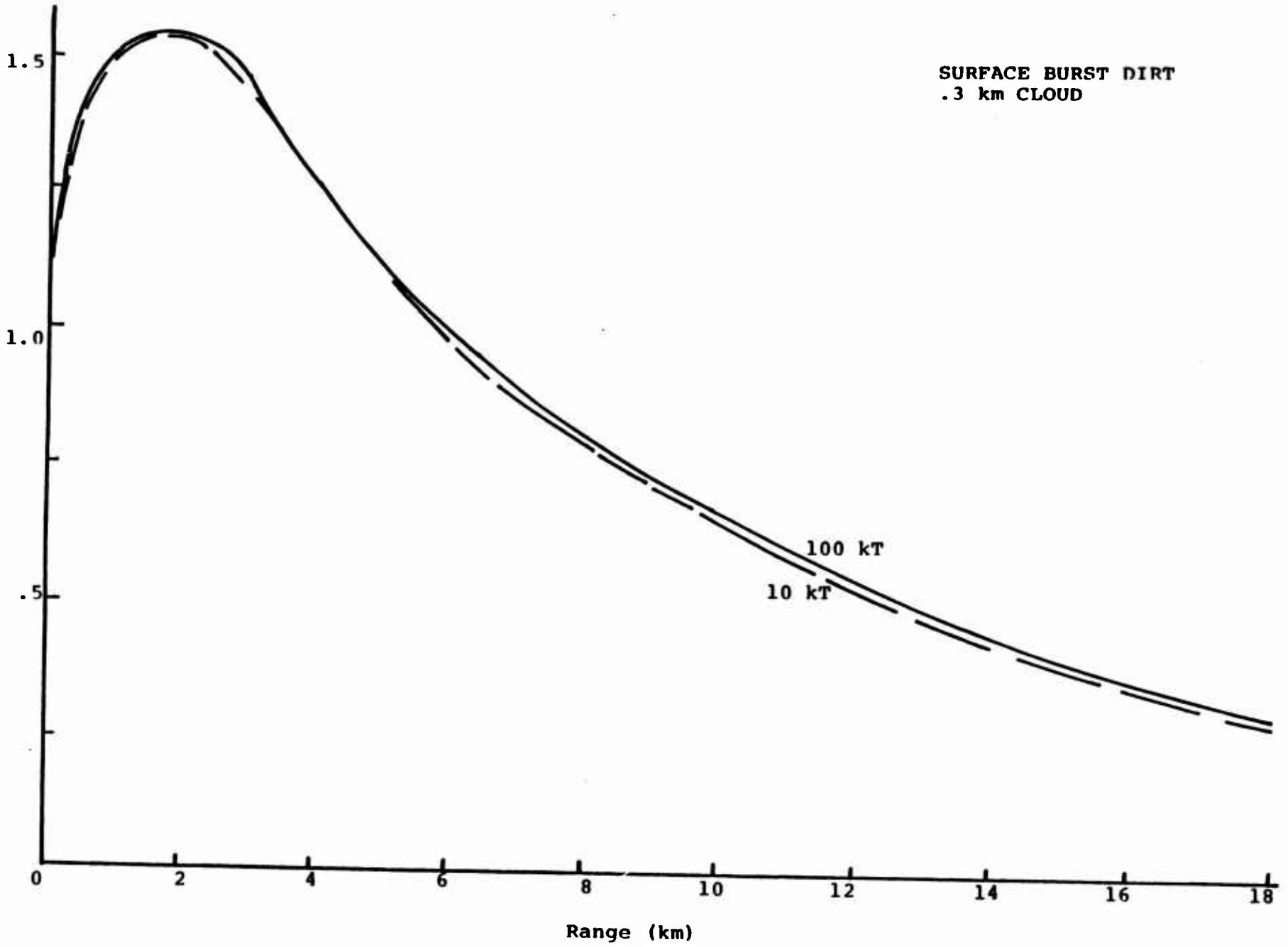

Figure 37. Effect of Yield on Transmission Predictions.

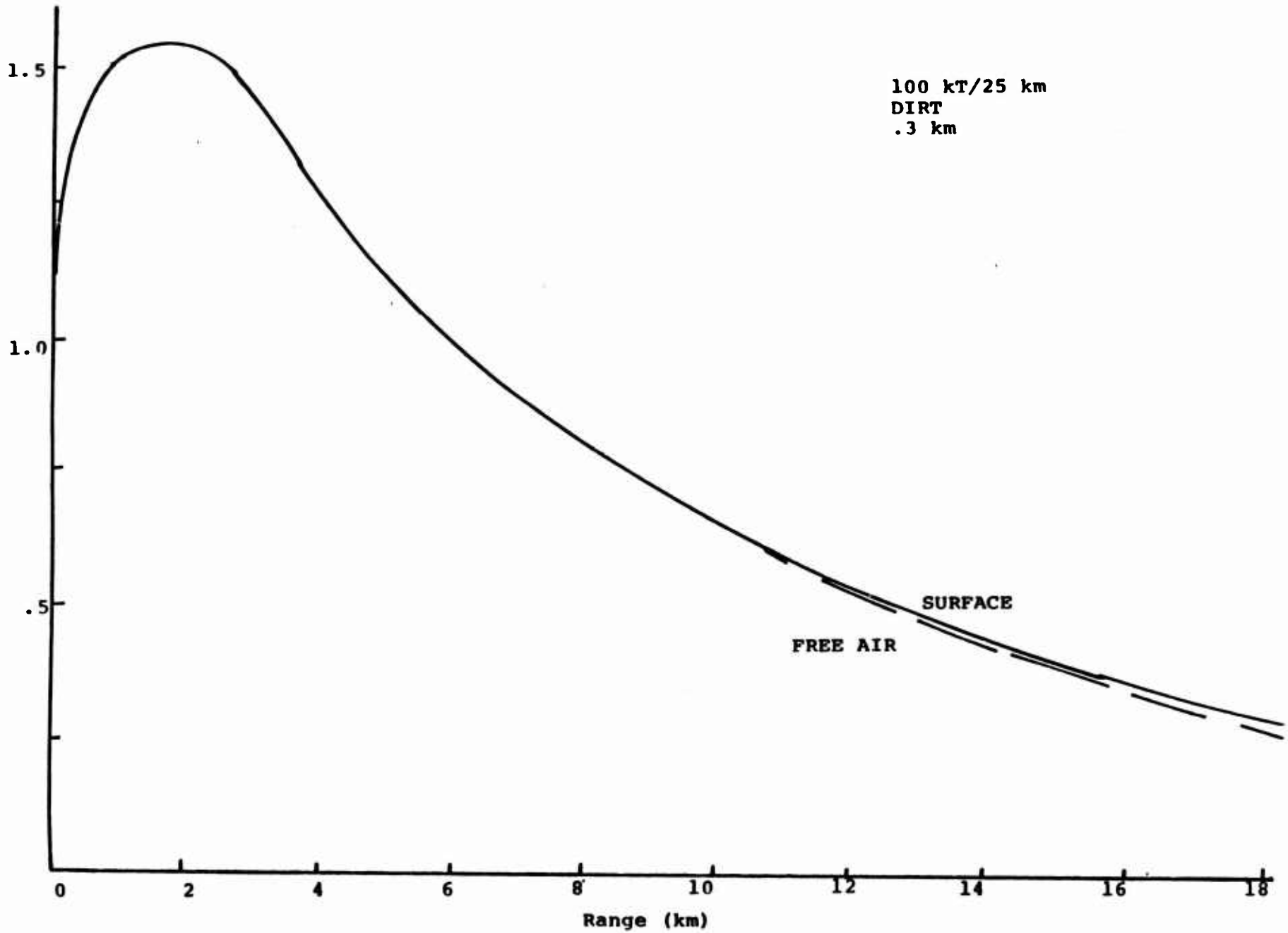

Figure 38. Effect of Spectrum Differences Caused by Surface Interactions on Transmission.

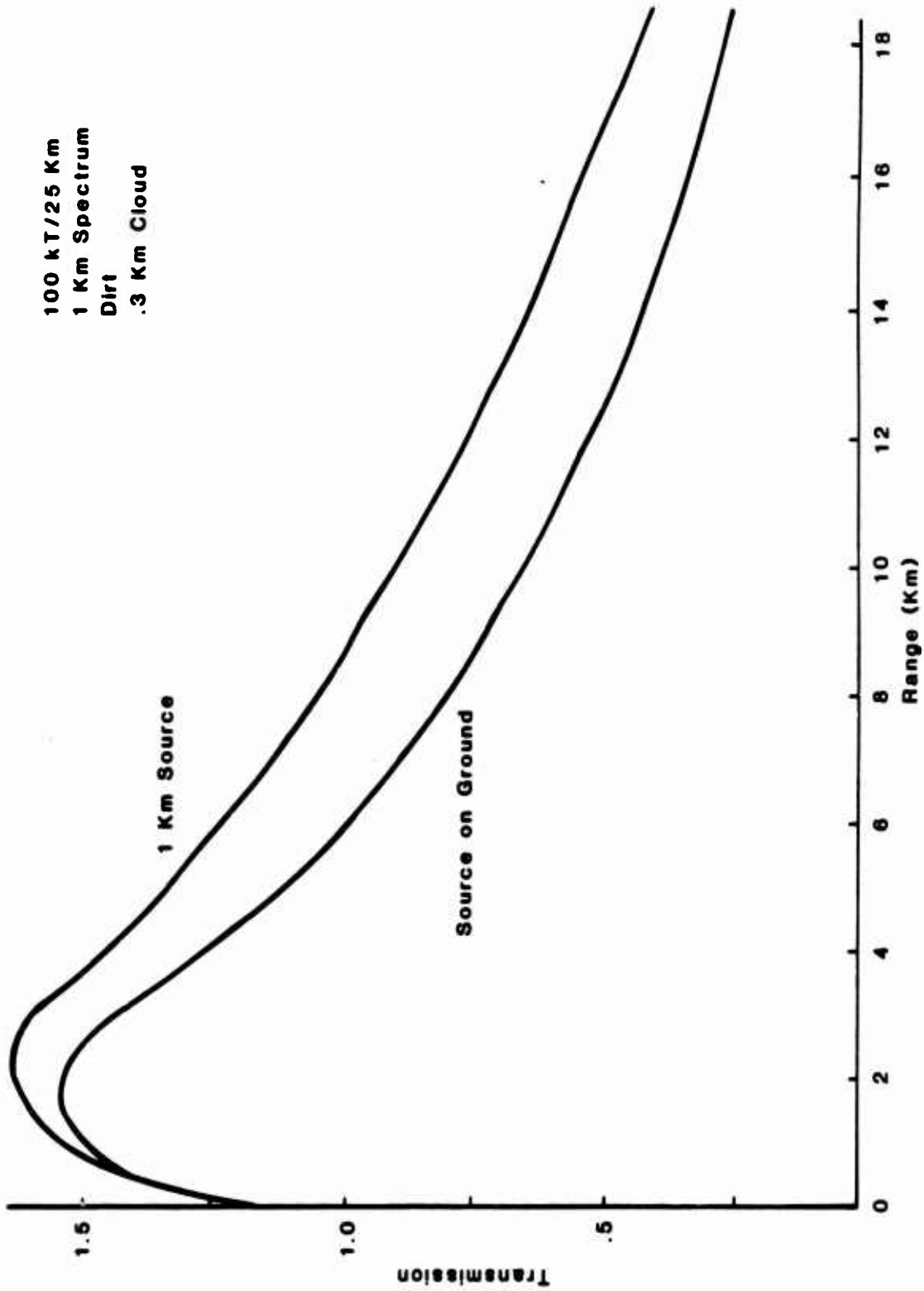

Figure 39. Effect of Source Altitude on Transmission Predictions.

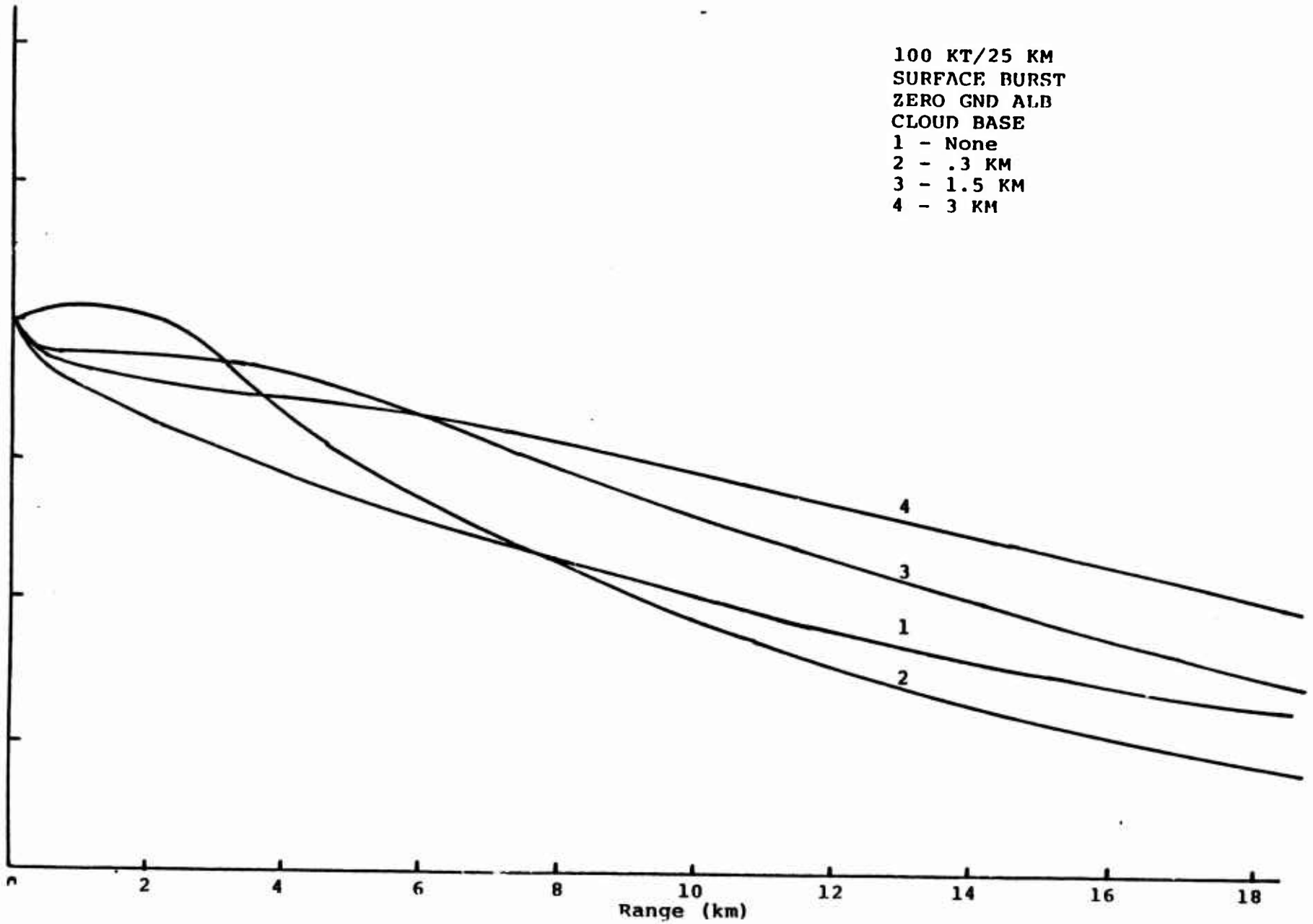

Figure 40. Effects of Cloud Ceiling Altitudes on the Transmission for Zero Ground Albedo.

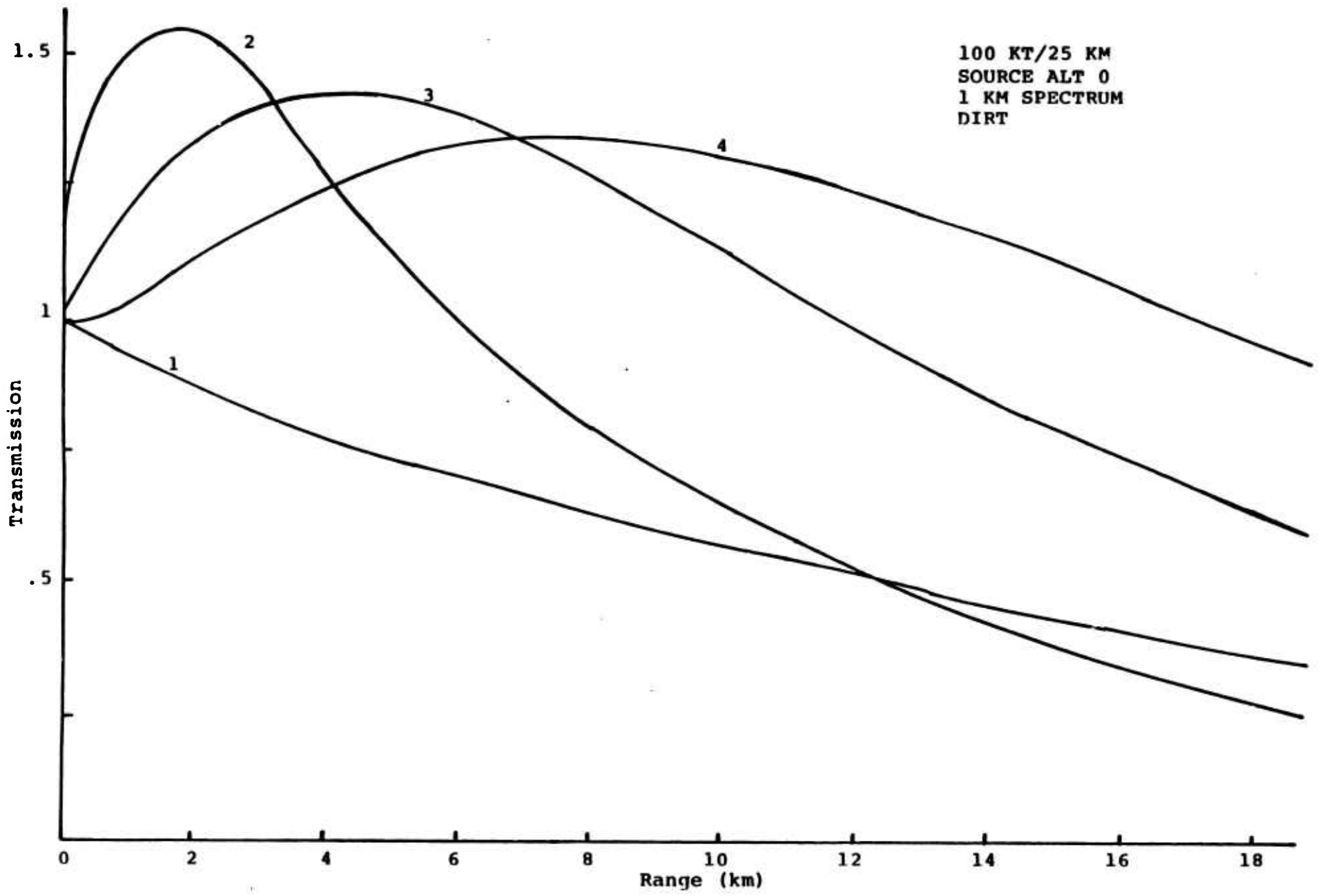

Figure 41. Effect of Cloud Ceiling Altitude on the Transmission for Dirt Ground Surface.

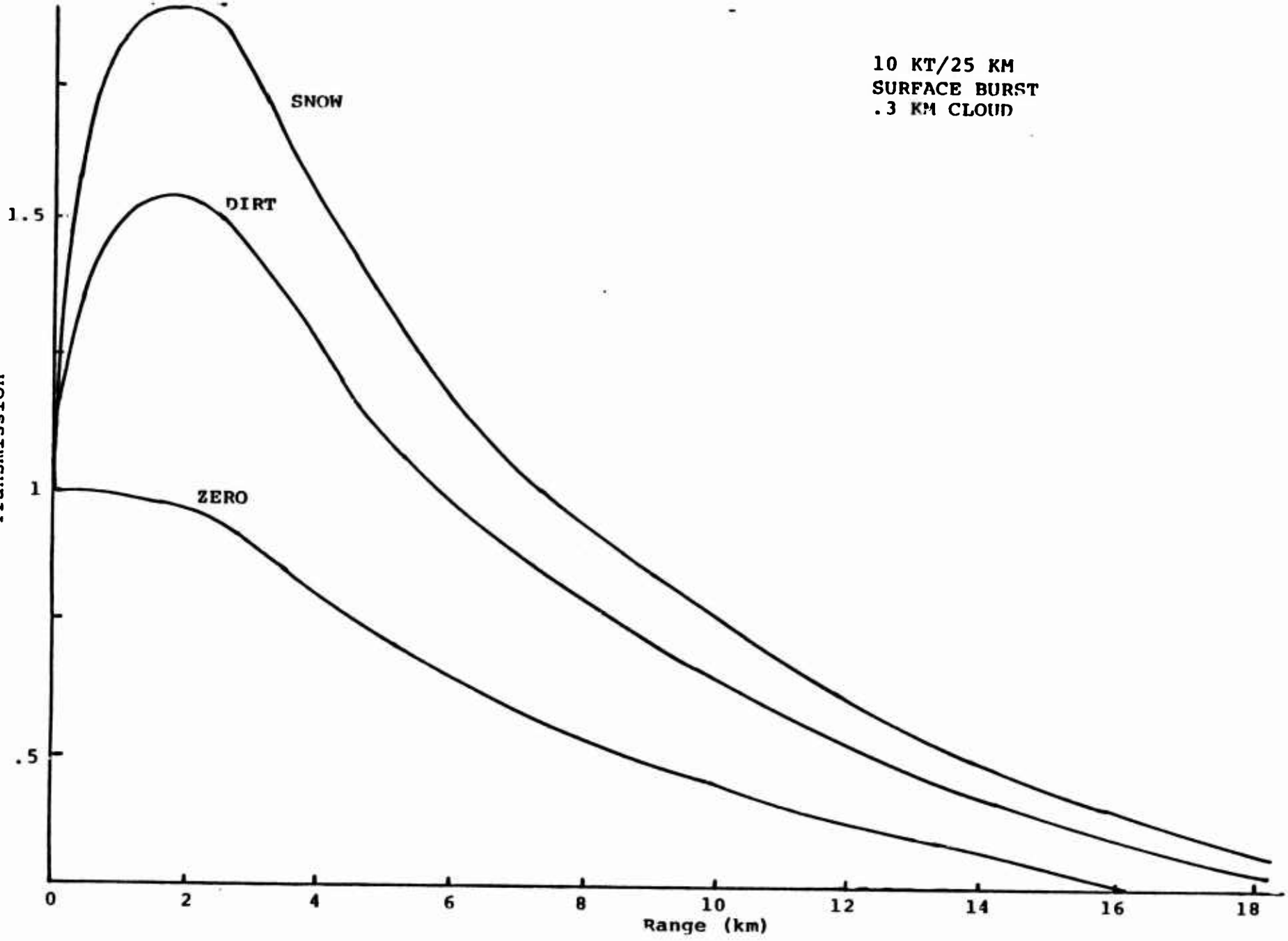

Figure 42. Effect of Ground Albedo on the Transmission.

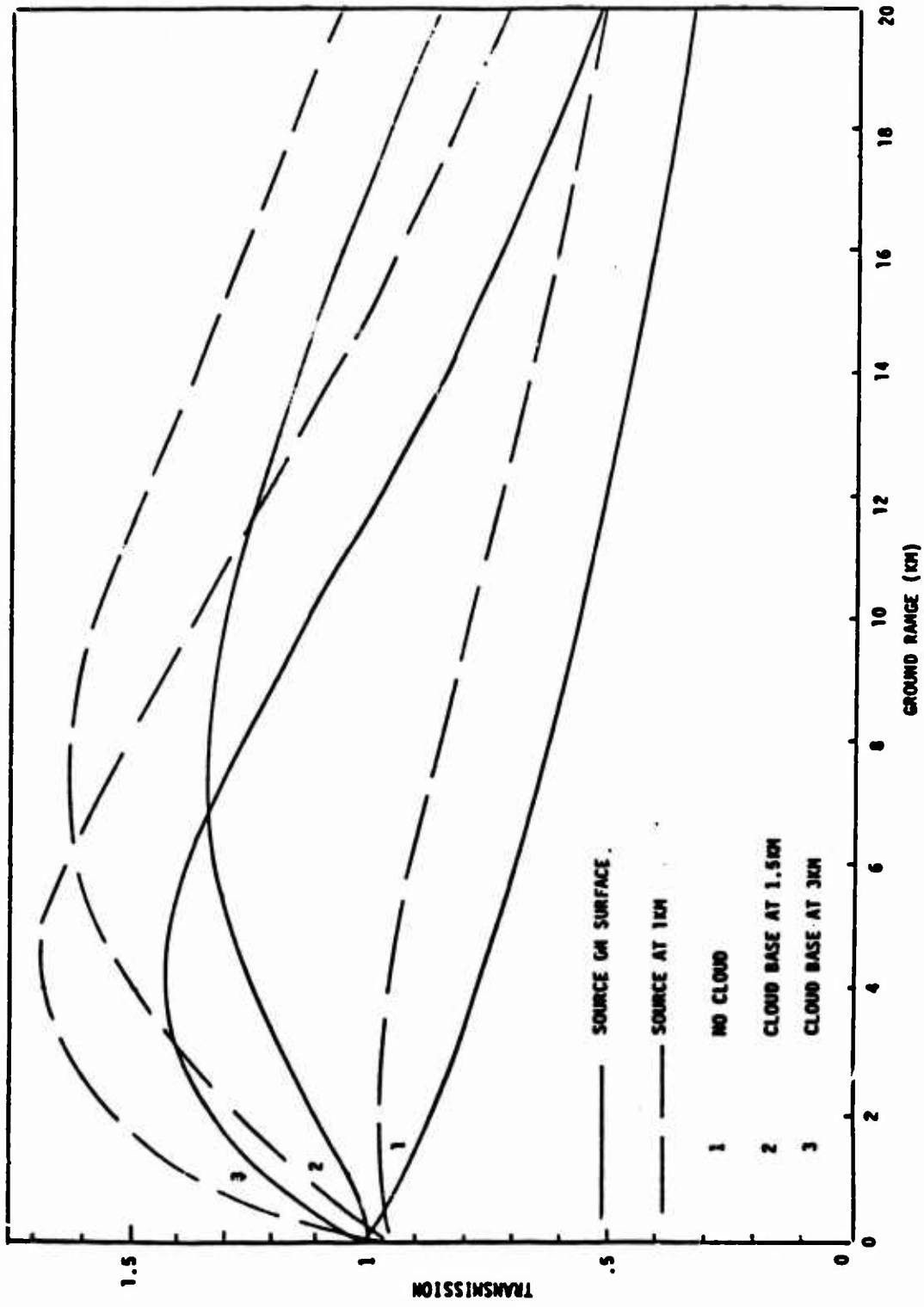

Figure 43. Effect of Burst Altitude on Transmission with Albedo Surfaces.

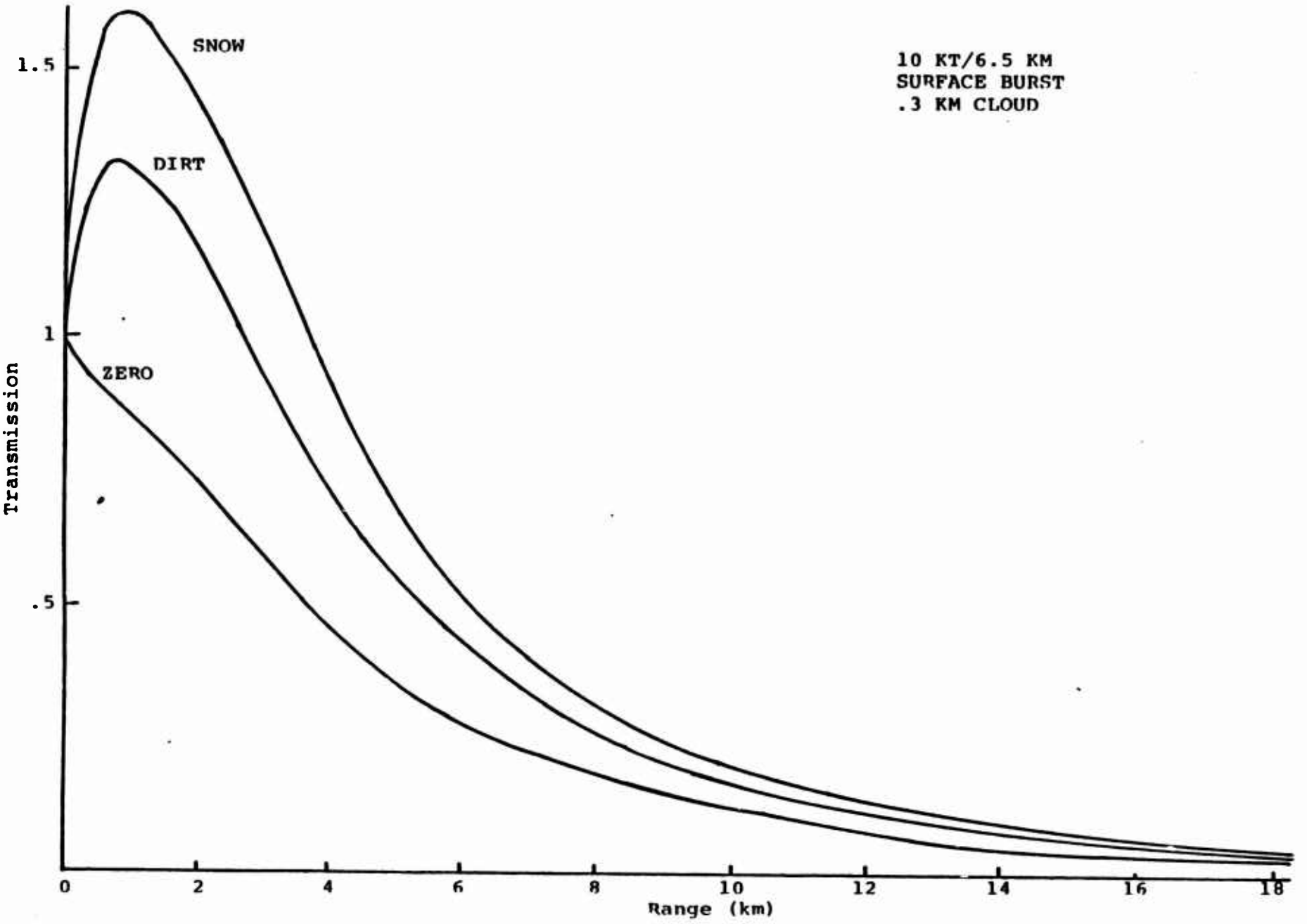

Figure 44. Effect of Surface Albedo for 6.5 km Visibility.